



Titania-based molecularly imprinted polymer for sulfonic acid dyes prepared by sol–gel method

Man Li, Rong Li*, Jin Tan, Zi-Tao Jiang*

Tianjin Key Laboratory of Food Biotechnology, College of Biotechnology and Food Science, Tianjin University of Commerce, Tianjin 300134, People's Republic of China

ARTICLE INFO

Article history:

Received 10 November 2012

Received in revised form

8 January 2013

Accepted 9 January 2013

Available online 17 January 2013

Keywords:

Titania

Molecularly imprinted polymer

Sol–gel process

Sulfonic acid dyes

Solid-phase extraction

ABSTRACT

A novel titania-based molecularly imprinted polymer (MIP) was synthesized through sol–gel process with sunset yellow (Sun) as template, without use of functional monomer. MIP was used as a solid-phase extraction material for the isolation and enrichment of sulfonic acid dyes in beverages. The results showed that MIP exhibited better selectivity, higher recovery and adsorption capacity for the sulfonic acid dyes compared to the non-imprinted polymer (NIP). MIP presented highest extraction selectivity to Sun when pH less than or equal to 3. The adsorption capacity was 485.9 mg g^{-1} , which was larger than that of NIP (384.7 mg g^{-1}). The better clean-up ability demonstrated the capability of MIP for the isolation and enrichment of sulfonic acid dyes in complicated food samples. The mean recoveries for the sulfonic acid dyes on MIP were from 81.9% to 97.2% in spiked soft drink.

© 2013 Elsevier B.V. All rights reserved.

1. Introduction

Food color is an important factor in the sensory quality of foodstuffs. To improve the sensory quality, food dyes have been added into food as a kind of additives. The dyes can be divided into two categories: natural and synthetic ones. Natural dyes are expensive because of their complex extraction processes. Due to the relatively simple refining method, synthetic food dyes are inexpensive, which increases their utilization in the food industry. However, the excessive consumption will cause great damage to body, especially to the liver, and even lead to organ malformations and carcinogenic [1]. So far, mostly used food dyes are sulfonic acid dyes such as tartrazine (Tar), sunset yellow (Sun), amaranth (Ama), brilliant blue (Bri), and ponceau 4R (Pon), whose structures are shown in Fig. 1.

Several methods have been developed for the screening and quantification of food dyes including high performance liquid chromatography [2,3], capillary electrophoresis [4], thin-layer chromatography [5], and spectrophotometry [6]. Nevertheless, it is essential for the complex samples to be treated before analysis because of impurities. Due to the high selectivity and affinity to the template molecule and its structural analogues, molecularly imprinted polymer (MIP) has been widely used in medicine [7,8], food [9,10] and environment analyses [11,12] as solid-phase

extraction (SPE) materials. Nowadays the main methods to synthesize molecularly imprinted materials are grafting procedures [13], precipitation polymerization [14], suspension [15], swelling polymerization [16], and surface imprinting on the spherical polymer or silica [17]. However, these methods are complex and also suffer from the choice of the functional monomer.

In the present work, a novel titania-based MIP was synthesized through sol–gel process with Sun as template, without adding functional monomer and cross-linker. Because of the strong polarity of the sulfonic acid group in the molecular structure of Sun, the coordination bond was formed easily between the titanium and Sun under acidic conditions. After the template was eluted, the hole that was similar to Sun, left in MIP which possessed high selectivity and affinity to the sulfonic acid dyes and could be used to extract them in beverages.

2. Materials and methods

2.1. Instrumentation

A model B203 biological microscope (Chongqing Optical Instrument Co. Ltd., China) was used to observe morphology in the drying process. A model SS-550 scanning electron microscope (SEM, Shimadzu Ltd., Japan) was used to observe the μm -range morphology of MIP and non-imprinted polymer (NIP). A model U-3900 UV diffuse reflectance spectroscopy (Hitachi Ltd., Japan) was used to record absorbance of MIP with barium sulfate pellets in transmission mode. A model F-Sorb 3400 surface analyzer

* Corresponding authors. Tel.: +86 22 26669671; fax: +86 22 26669670.

E-mail addresses: lirong@tjcu.edu.cn (R. Li), ztjiang@yahoo.com, ztjiang@tjcu.edu.cn (Z.-T. Jiang).

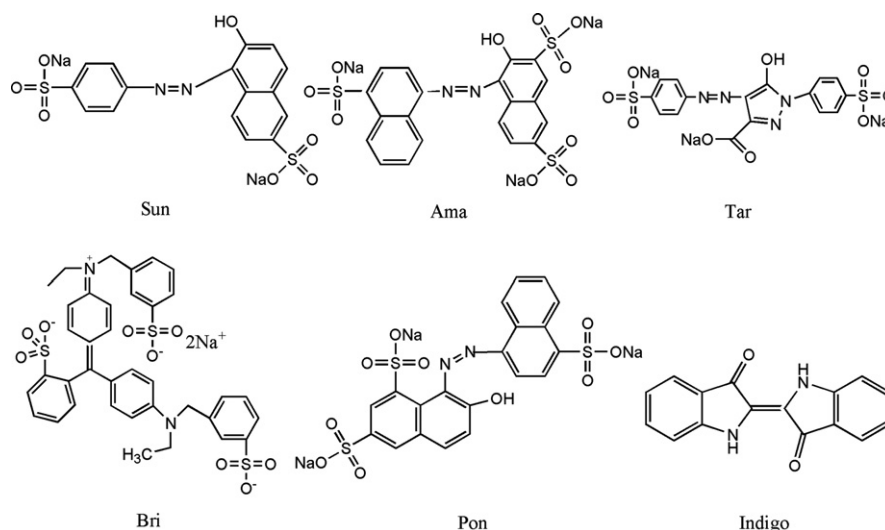


Fig. 1. The molecular structures of six food dyes.

(APP. Co. Ltd., China) was used to measure specific surface area and pore size distribution of MIP. HPLC analysis was performed on the Agilent 1100 series HPLC system containing a G1322A vacuum degasser, a G1312A binary pump, a G1313A ALS autosampler a G1316A column compartment and a G1315B diode array detector. Separation was carried out on a Zorbax SB-C18 column (250 mm \times 4.6 mm i.d., particle size 5 μ m).

2.2. Materials and chemicals

Titanium isopropoxide ($\text{Ti}(\text{O}^i\text{Pr})_4$) as a precursor was purchased from Taichang Chemical Co., Ltd. (Tianchang, China). Acetic acid (HAc, 99%) and hydrochloric acid (HCl, 36–38%) were obtained from Tianjin No. 1 Chemical Reagent Co. (Tianjin, China). Sun, Ama, Tar, Bri, Pon, and indigo were obtained from Tianjin Guangfu Fine Chemical Research Institute (Tianjin, China). Methanol was of HPLC grade and procured from Kermel (Tianjin Chemical Reagent Co., Ltd. China). Milli-Q purification water was obtained from Milli-Q purification system (Millipore, USA) and used throughout all experiments.

2.3. Synthesis process of MIP

Aliquots of 1.74 mL of HAc and 2.84 g of $\text{Ti}(\text{O}^i\text{Pr})_4$ were mixed under stirring condition for 30 min. After 0.55 mL of concentration HCl was added for about 30 min, 3.25 mL of Sun aqueous solution was added to the mixture under vigorous stirring for 30 min. Then, the homogeneous solution was poured into a glass tube, sealed and allowed to gel at ambient temperature. In this method, the amount of template and the drying conditions should be taken into consideration. NIP was prepared in the same way but without the template.

2.4. Static binding studies

An amount of 10 mg of MIP particles was weighed and then put into 10 mL of Sun standard aqueous solution an appropriate concentration, slightly oscillated for 12 h at room temperature in the dark, and then centrifuged at 4000 rpm for 15 min. The concentration of free Sun in the supernatant was determined by visible spectrophotometry at 482 nm wavelength. The amount of Sun bound into MIP particles was calculated by subtracting the amount of free Sun from the initial amount added to the mixture. The adsorption capacity (Q , mg g^{-1}) proposed for the characterization

of the adsorption ability was applied to examine the adsorption abilities of MIP and NIP [17].

$$Q = \frac{(C_o - C_e)VM}{W} \quad (1)$$

where C_o (mmol L^{-1}) is the initial concentration, C_e (mmol L^{-1}) is the final concentration after extraction, V (mL) is the volume of solution, W (g) is the weight of MIP or NIP, and M (g mol^{-1}) is the molar mass of sulfonic acid dyes

Distribution and selectivity coefficients of sulfonic acid dyes were calculated as explained below [18]:

$$K_D = \frac{C_o - C_e}{C_e} \quad (2)$$

where K_D represents the distribution coefficient, the selectivity coefficient (K) for the binding of sulfonic acid dyes in the presence of competitor can be obtained from equilibrium data according to Eq. (3) [18].

$$K = K_{D1}/K_{D2} \quad (3)$$

where K_{D1} is the distribution coefficient of the template molecule and K_{D2} is the distribution coefficient of competitor.

2.5. Dyes of extraction by MIP from beverages

Different beverage samples were pretreated with different methods. The carbonated drinks were degassed by ultrasound before use, and the juice drink containing flesh was filtered. Then, 1 mL of sample solution was diluted to 10 mL and in the process pH-value of the solution was adjusted to pH 3. In order to evaluate the adsorption ability of MIP to sulfonic acid dyes from the sample solution, 20 mg of the MIP was added into the prepared sample solution. The mixture was slightly oscillated for 5 h at room temperature in the dark. The mixture was centrifuged and the supernatant was thrown away. MIP-containing dyes were washed three times by distilled water. Finally, 3.0 mL 1% $\text{NH}_3 \cdot \text{H}_2\text{O}$ was used to elute the extracted dyes. The eluent was collected and introduced to HPLC.

2.6. HPLC analysis

The mobile phase was the mixture of methanol (A) and ammonium acetate aqueous solution (B). The content of A was increased linearly from 12% to 15% in the first 7 min, from 15% to

40% from 7 min to 9 min, and then held for 40% to the end. The concentration of ammonium acetate was 20 mmol L^{-1} thoroughly. The flow rate of 1.0 mL min^{-1} and UV detector wavelength was set at 254 nm.

3. Results and discussion

3.1. Preparation of MIP

3.1.1. Mechanism of reaction

In this synthesis process, CH_3COO^- of HAC as a ligand group could partly substitute the isopropoxy of $\text{Ti}(\text{O}^i\text{Pr})_4$, which would weaken the speed of hydrolysis and polycondensation of $\text{Ti}(\text{O}^i\text{Pr})_4$. HCl as the hydrolysis reaction catalyst could promote the speed of the residue of isopropoxy substituted by hydroxy. Because of the higher polarity of sulfonic acid groups of Sun, it could substitute the CH_3COO^- through coordination bond. With the polycondensation, the titania-based MIP was synthesized through a sol-gel process. After the template rinsed by ammonia, MIP would be imprinted with the hole that was similar to the template molecule. The principle of synthesis process of MIP is shown as Fig. 2.

3.1.2. Selection of the amount of template and drying condition

In order to obtain MIP with good imprinted efficiency, some factors have to be thought. These factors include the amount of template and drying condition after the formation of sol. First, an appropriate amount of template was very important. The maximum solubility of Sun in 3.25 mL water is 1.4 mmol. Therefore, 0.1 mmol, 0.2 mmol, 0.5 mmol, 1 mmol, and 1.4 mmol of template were chosen to discuss the effect on imprinted efficiency. Based on the results of UV diffuse reflectance spectroscopy (Fig. 3), the absorbance of MIP

increased rapidly with the increase of the amount of template in low concentrations. However, when the amount was more than 1 mmol, the absorbance virtually unchanged. So the amount of template was chosen as 1 mmol.

Fig. 4 shows the microscope images of the gel of MIP in different drying conditions (the initial temperature was 30°C , 60°C and 80°C , respectively). As shown, the particles increased with the increase of temperature and tended to sphere. The gel time decreased from 120 min to 15 min. However, for NIP, the gel time was up to 24 h and the gel mainly occurred in the bottom of

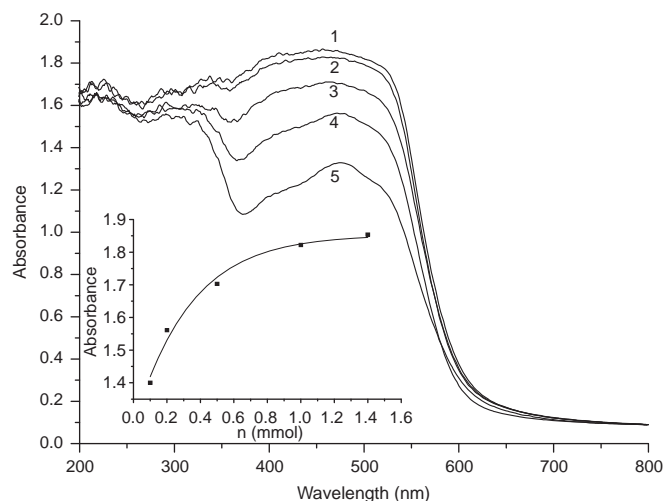


Fig. 3. Ultraviolet diffuse reflection spectra of MIP with different amount of template. From 1 to 5 the amounts of template were 1.4 mmol, 1.0 mmol, 0.5 mmol, 0.2 mmol, 0.1 mmol, respectively, Inset is the absorbance of different materials at 480 nm.

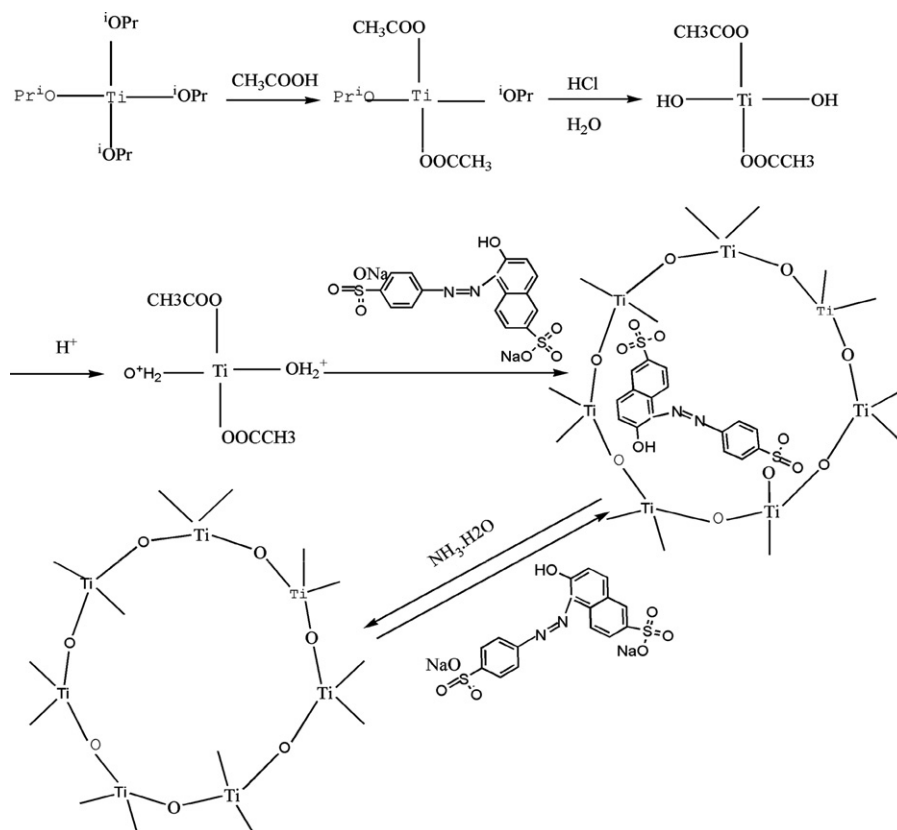


Fig. 2. Synthesis principle of MIP.

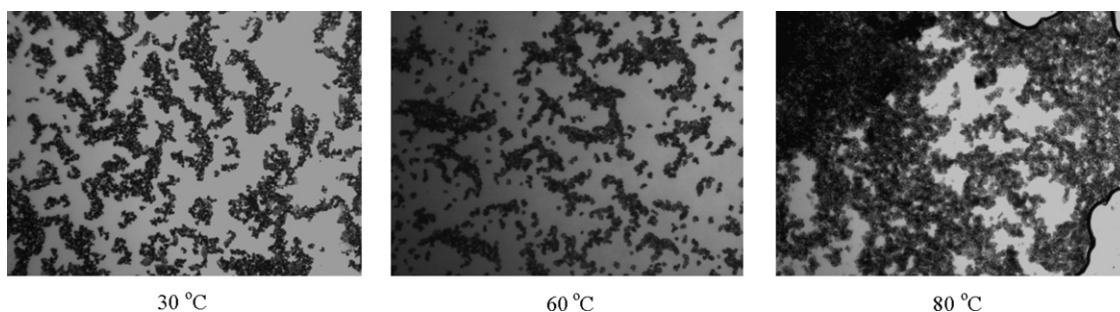


Fig. 4. Microscope images of the gel of MIP in different initial temperature, the left is 30 °C, the middle is 60 °C, the right is 80 °C.

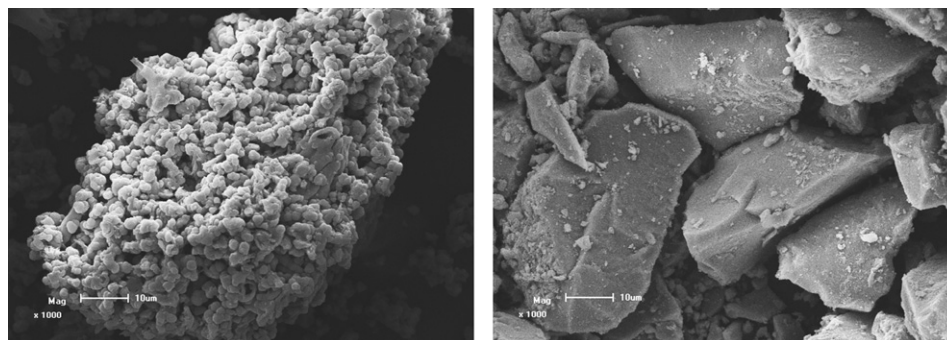


Fig. 5. SEM of MIP (left) and NIP (right) under the magnification 1000.

the tube when it was placed into a 30 °C incubator at initial time. When the temperatures were 60 °C and 80 °C, the macro-structure of the gel systems were changed from asymmetric to homogeneous particles but the specific surface area decreased. The some reasons for the above phenomenon might be that in the low temperature, the titanium dioxide particles moved at a low speed, which decreased the probability of collisions between the particles and the gel time became longer. With the increase of temperature, the probability of collisions between the particles increased and the polycondensation took place. In summary, the sol was placed into 60 °C oven directly for 3 days, then 80 °C for 3 days, 100 °C for 2 days, and 120 °C for 1 day, which was identified as the final drying conditions.

3.2. The characteristic of MIP

3.2.1. SEM of MIP

Morphology of MIP and NIP was obtained by SEM (Fig. 5). Fig. 5 shows obvious difference between MIP and NIP. The particles of NIP were much smaller than those of MIP and also no macro- and mesoporous structures which distributed obviously in MIP. The specific surface area, average pore diameter, and cumulative pore volume of MIP were $126.68 \text{ m}^2 \text{ g}^{-1}$, 12.32 nm and 0.39 mL g^{-1} , respectively. However, these surface parameters were $110.60 \text{ m}^2 \text{ g}^{-1}$, 10.68 nm and 0.29 mL g^{-1} for NIP. From the results, it can be inferred that during the synthesis of the materials Sun was involved in the reaction as a porogen.

3.2.2. UV diffuse reflectance spectroscopy

The UV diffuse reflectance spectra of Sun, MIP, NIP and the mixture of NIP and Sun are shown in Fig. 6(A–D). As shown, Sun had strong absorbance at the wavelength of 380 nm–550 nm. NIP presented photoabsorption properties at the UV light region. However, the UV diffuse reflectance spectrum of the mixture of NIP and Sun showed neither absorption peak movement nor new band, which indicated that no chemical effects occurred between

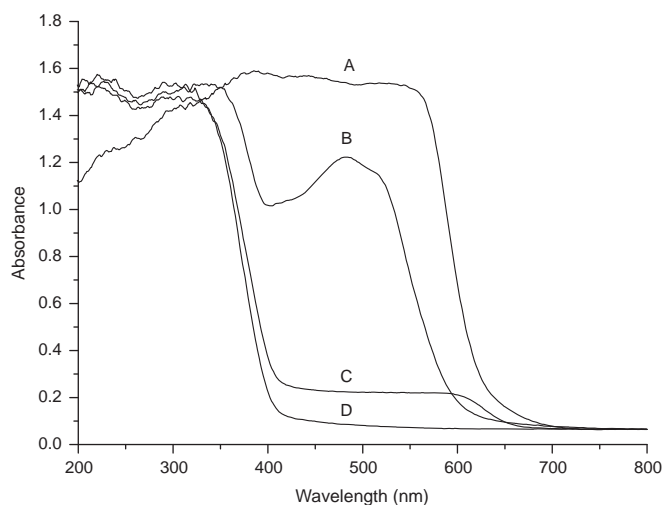


Fig. 6. Ultraviolet diffuse reflection spectrum diagram of different materials. (A) Sun power. (B) MIP. (C) The mixture of NIP and Sun power. (D) NIP.

them. In the UV diffuse reflectance spectrum of MIP, a new absorption peak appeared at 480 nm indicating that Sun had been involved in the reaction to synthesize MIP. Meanwhile, because of the addition of template molecule the polarity of titania changed and led to the characteristic absorption peaks of titania red-shift, which led to a change of the structure of Sun.

3.3. Sorption ability of MIP

3.3.1. Effect of pH

The pH is one of the most important parameters controlling the sorption process. In order to investigate the effect of pH on the adsorption characteristics of MIP and NIP, the pH-values of solution were adjusted to 2, 3, 4, 5, and 6, respectively. The effect

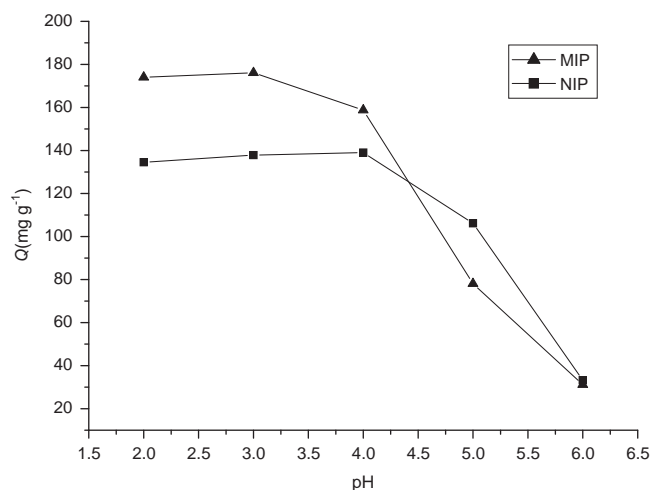


Fig. 7. Effect of pH on the static adsorption of Sun on MIP and NIP. Analyte: 0.5 mmol L⁻¹ 10 mL Sun aqueous water at different pH.

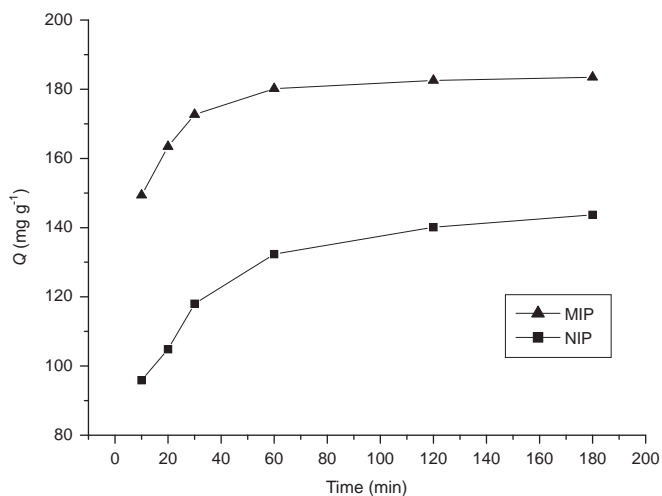


Fig. 8. Adsorption time curves of MIP and NIP to 0.5 mmol L⁻¹ Sun aqueous solution in pH 3.

of pH is shown in Fig. 7. When pH was between 5 and 6, the adsorption capacity of MIP and NIP was weak. The reason might be that in this pH range, electrostatic repulsion between the surface of titania and Sun played a dominant role, which weakened the combination between them. With the decrease of the solution pH, the adsorption capacities of MIP and NIP increased. The adsorption capacity was up to the balance when pH was below 3 and also in this range of pH between 2 and 4 the adsorption capacity of MIP to Sun was greater than NIP. That is because with the decrease of pH, the specific adsorption between MIP and Sun increased, however, the adsorption capacity increased less for NIP due to the lack of the specific holes.

3.3.2. Adsorption kinetics

The adsorption kinetics is an important indicator of the adsorbent efficiency. The adsorption kinetics was investigated with 0.5 mmol L⁻¹ Sun aqueous solution. As shown in Fig. 8, the adsorption capacity reached 80% of the equilibrium value within 30 min after the addition of Sun and the equilibrium time was about 60 min for MIP. And also compared with NIP the adsorption capacity of MIP was higher at the same concentration.

In order to further study the adsorption kinetics of MIP to Sun, the pseudo first-order equation (Eq. (4)) and the pseudo second-order equation (Eq. (5)) were selected in this experiment for describing the adsorption kinetics [19].

$$\log(Q_e - Q_t) = \log Q_e - k_1 t / 2.303 \quad (4)$$

$$\frac{t}{Q_t} = \frac{1}{k_2 Q_e^2} + \frac{t}{Q_e} \quad (5)$$

where Q_e and Q_t are the amount of Sun adsorbed (mg g⁻¹) on the adsorbent at the equilibrium and at time t , respectively, and k_1 is the rate constant of adsorption (L min⁻¹). Values of k_1 were calculated from the plots of $\log(Q_e - Q_t)$ versus t ; and k_2 is the rate constant of pseudo second-order adsorption (g mg⁻¹ min⁻¹). The constant k_2 can be obtained from plotting (t/Q_t) versus t . The values of k_1 and k_2 , correlation coefficients (R) are given in Table 1.

The experimental data for the adsorption of Sun onto MIP and NIP treated with the above-mentioned kinetic models were used to evaluate the controlling mechanism of adsorption processes. According to the data in Table 1, the higher R values confirmed that the adsorption data were well represented by pseudo second-order kinetics for the entire adsorption period. So it is inferred that the adsorption is a chemical adsorption process. The values of the second-order rate constants (k_2) were 0.0024 g mg⁻¹ min⁻¹ and 0.0009 g mg⁻¹ min⁻¹ for MIP and NIP, respectively, which indicated that the adsorption rate of MIP was higher than NIP.

3.3.3. Adsorption isotherm

To estimate the adsorption capacity of Sun on the MIP and NIP, an adsorption experiment was carried out under pH 3 at room temperature (temperature has nothing to do with the absorption capacity in this work) by comparing the adsorption of different concentrations of Sun on the MIP and NIP. The adsorption capacities of Sun by the MIP and NIP are represented in Fig. 9. It is clear

Table 1

The pseudo first-order and second-order kinetic parameters for Sun on MIP and NIP.

Absorbent	First-order kinetics		Second-order kinetics	
	k_1	R	k_2	R
MIP	0.0175	0.9406	0.0022	0.9999
NIP	0.0223	0.9959	0.0009	0.9998

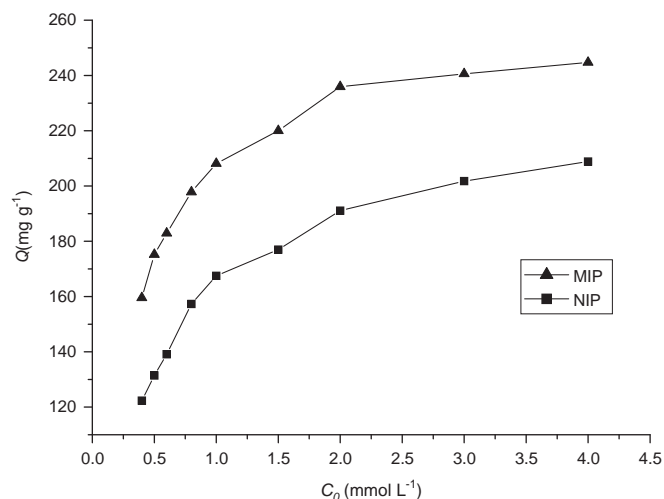


Fig. 9. Binding isotherm for MIP and NIP to increasing concentrations of Sun in 10 mL water at pH 3 at room temperature.

that both MIP and NIP showed an increase in binding amounts as the initial concentration increased. NIP showed high adsorption capability to Sun and the reason might be that titania possessed strong adsorption ability to electronegative substance under acidic condition. However, MIP exhibited a higher capacity for Sun than NIP because of the imprinting effect.

After the isotherm adsorption experiments, the data obtained were linearized with Langmuir (Eq. (6)) [20] and Freundlich (Eq. (7)) [21] according to the following equation:

$$\frac{C_e}{Q_t} = \frac{C_e}{Q_m} + \frac{k_d}{Q_m} \quad (6)$$

where Q_m is the monolayer adsorption capacity (mg g^{-1}) and k_d is the constant related to the free adsorption energy (Langmuir constant, mmol L^{-1}).

$$\log Q = \frac{1}{n} \log C_e + \log K_F \quad (7)$$

where K_F is a constant indicative of the adsorption capacity of the adsorbent (mg g^{-1}) and the constant n indicates the intensity of the adsorption.

According to the results, the Freundlich isotherm model had higher values of regression coefficients when compared to the Langmuir isotherm models, which showed the multilayer nature of the adsorbent. For MIP, the linear relationship is $y = 2.6865 + 0.10432x$ ($R = 0.995$), K_F and n could be calculated from the slope and intercept which were 485.9 mg g^{-1} and 9.6 mg g^{-1} , respectively. For NIP the linear relationship is $y = 2.58512 + 0.1667x$ ($R = 0.992$), K_F and n were 384.68 mg g^{-1} and 6.0 mg g^{-1} , respectively, which were lower than MIP.

3.3.4. Selectivity of MIP

According to experimental procedure in Section 2.4, the initial concentrations of sulfonic acid dyes were 0.5 mmol L^{-1} , the adsorption capacities of MIP and NIP are shown as Fig. 10.

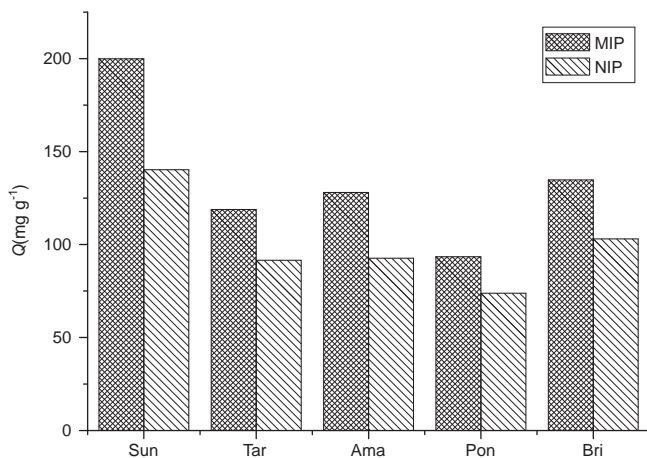


Fig. 10. The absorption capacity of Tar, Sun, Ama, Bri, Pon on MIP and NIP separately to the initial concentration of each kind of sulfonic acid dyes was 0.5 mmol L^{-1} .

Table 2

Distribution and selectivity coefficient of Sun in the mixture for MIP and NIP.

Mixture		C_p		C_e		K_D		K	
		NIP	MIP	NIP	MIP	NIP	MIP	NIP	MIP
Tar/Sun	Tar	0.0978	0.1212	0.3032	0.2788	0.3326	0.4347	1.90	1.76
	Sun	0.1573	0.1734	0.2427	0.2266	0.6333	0.7652		
Ama/Sun	Ama	0.0894	0.1364	0.3106	0.2636	0.2878	0.5174	2.43	1.36
	Sun	0.1646	0.1649	0.2352	0.2351	0.6998	0.7014		

The results showed that both MIP and NIP can adsorb sulfonic acid dyes. But compared with NIP, MIP had greater adsorption capacity. To investigate the selectivity of MIP among sulfonic acid dyes, the competitive adsorption experiments were conducted by preparing a mixture of Sun and Tar, Sun and Ama, in which each dye of the initial concentration was 0.4 mmol L^{-1} . The C_p , C_e , K_D and K are given in Table 2. It was shown that the adsorption capacities of MIP to Sun and its structural analogues were higher than those of NIP. However, compared with Sun, MIP was easier to combine with Tar and Ama. The reason might be that the carboxyl and sulfonic acid group could increase the binding force between the dyes and MIP.

The competitive adsorption of MIP between sulfonic acid dye and non-sulfonic acid dye was conducted by MIP's selectively extracting Sun from a mixture of Sun and indigo (non-sulfonic acid dye), in which the initial concentration of both dyes were 0.4 mmol L^{-1} . The result showed that MIP adsorbed selectively Sun in the presence of indigo. That is because there is no sulfonic acid group in the molecular structure of indigo, so the coordination bond cannot form between sulfonic acid group and titanium ion. In addition, the geometry and space size between MIP and indigo did not match each other, which was also a very important factor.

3.4. Linearity, accuracy, limit of detection (LOD), and limit of quantification (LOQ)

The HPLC method presented good linearities to sulfonic acid dyes in the range of $0.002 \text{ mmol L}^{-1}$ – 0.2 mmol L^{-1} . The linearity correlation coefficient (R) was about 0.999 for these four kinds of sulfonic acid dyes. The repeatability and accuracy were evaluated by analyzing spiked beverage samples with $2 \mu\text{mol L}^{-1}$, $4 \mu\text{mol L}^{-1}$, and $6 \mu\text{mol L}^{-1}$ for each sulfonic acid dye. The results are summarized in Table 3. The recoveries of four kinds of sulfonic acid dyes by MIP cartridges ranged from 81.9% to 97.2%. The limits of detection (LOD) were $0.36 \mu\text{mol L}^{-1}$ for Sun, $0.18 \mu\text{mol L}^{-1}$ for Tar, $0.13 \mu\text{mol L}^{-1}$ for Ama, and $0.32 \mu\text{mol L}^{-1}$ for Pon, respectively. The limits of quantification (LOQ) were $1.20 \mu\text{mol L}^{-1}$ for Sun, $0.60 \mu\text{mol L}^{-1}$ for Tar, $0.43 \mu\text{mol L}^{-1}$ for Ama, and $1.07 \mu\text{mol L}^{-1}$ for Pon, respectively.

Table 3

Recoveries (%) of four sulfonic acid dyes determined in spiked beverage at three concentration levels ($n=3$).

Sample	Spiked ($\mu\text{mol L}^{-1}$)	Sun		Ama		Pon		Tar	
		MIP	NIP	MIP	NIP	MIP	NIP	MIP	NIP
A	2	85.4	56.5	94.2	83.2	93.5	84.1	95.4	82.9
	4	84.6	58.8	93.7	81.5	92.6	83.2	94.6	82.6
	6	81.9	54.4	92.4	80.9	91.2	83.4	94.1	82.1
B	2	89.7	68.9	97.2	83.7	97.2	81.8	94.2	81.9
	4	89.4	65.4	96.5	82.5	96.9	81.5	93.9	81.2
	6	88.5	67.5	96.3	81.9	96.5	80.9	93.6	81.2
C	2	94.7	67.8	92.8	82.1	91.9	82.7	96.9	83.3
	4	93.6	68.2	92.6	80.9	91.3	82.1	96.2	82.7
	6	91.2	66.9	90.9	80.9	91.1	81.7	95.8	82.1

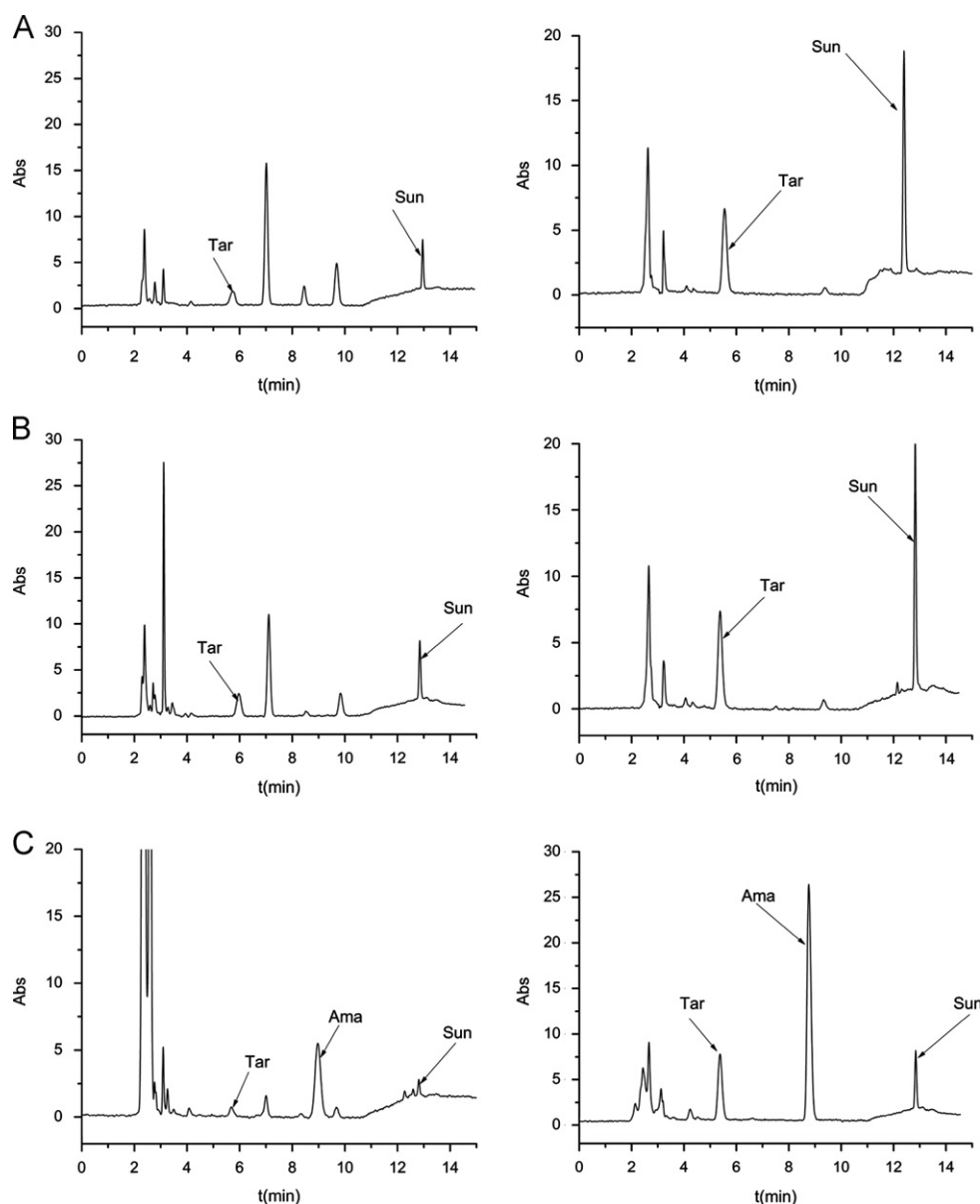


Fig. 11. Chromatograms of beverage sample A, B, C before (A-1, B-1, C-1) and after (A-2, B-2, C-2) the SPE based on MIP.

The relative standard deviations (RSD) were of 1.36–2.65%. Thus, MIP exhibited good selectivity for both the template and its structural analogues. This group-selective binding character of MIP would allow accurate quantification of Sun and its structural analogues.

3.5. Application of MIP in beverages

Using HPLC determination, we found that Sun and Tar existed in sample A, B and C. Besides two dyes, sample C also contained Ama and vitamin. As the result determined by HPLC, the contents of Sun and Tar were $1.6941 \text{ mg kg}^{-1}$ and $0.8602 \text{ mg kg}^{-1}$ in sample A, and $2.3573 \text{ mg kg}^{-1}$ and $1.1109 \text{ mg kg}^{-1}$ in sample B, respectively. The contents of Sun, Tar and Ama were $0.5618 \text{ mg kg}^{-1}$, $0.1645 \text{ mg kg}^{-1}$ and $2.3267 \text{ mg kg}^{-1}$ in sample C, which were within the scope of FDA regulation.

Fig. 11 shows chromatograms of sample A, B, and C before and after the SPE using MIP. By comparison with chromatograms of the same sample in the above-mentioned two conditions, we found that the beverage samples pretreated by MIP showed very clean

chromatographic trace and the peaks corresponding to Sun, Tar and Ama, which makes the sample analysis become more easily.

4. Conclusions

In this work, a titania-based MIP for sulfonic acid dyes by sol–gel method has been prepared. The MIP could be applied as a sorbent of sulfonic acid dyes in the beverage samples and exhibited excellent selectivity and affinity for sulfonic acid dyes. LODs for sulfonic acid dyes were between $0.13 \text{ } \mu\text{mol L}^{-1}$ and $0.36 \text{ } \mu\text{mol L}^{-1}$. MIP appeared to be well-suited tool to remove the interfering compounds and to enrich sulfonic acid dyes in beverage samples.

Acknowledgements

This work was supported by the Natural Science Foundation of Tianjin and the Science Foundation for Young Teachers of Tianjin University of Commerce.

References

- [1] S.W. Collier, J.E. Storm, R.L. Bronaugh, *Toxicol. Appl. Pharmacol.* 118 (1993) 73–79.
- [2] S.P. Alves, D.M. Brum, E.C.B. Andrade, N.A.D. Pereira, *Food Chem.* 107 (2008) 489–496.
- [3] N. Yoshioka, K. Ichihashi, *Talanta* 74 (2008) 1408–1413.
- [4] C.O. Thompson, V.C. Trenerry, B. Kemmery, *J. Chromatogr. A* 694 (1995) 507–514.
- [5] J.J. Nevado, C.G. Cabanillas, A.M. Salcedo, *Talanta* 41 (1994) 789–797.
- [6] J.J. Nevado, C.G. Cabanillas, A.M. Salcedo, *Talanta* 42 (1995) 2043–2051.
- [7] R.N. Rao, P.K. Maurya, S. Khalid, *Talanta* 85 (2011) 950–957.
- [8] Z.G. Xu, Y.F. Hu, Y.L. Hu, G.K. Li, *J. Chromatogr. A* 1217 (2010) 3612–3618.
- [9] M.M. Zheng, R. Gong, X. Zhao, Y.Q. Feng, *J. Chromatogr. A* 1217 (2010) 2075–2081.
- [10] S. Wang, Z.X. Xu, G.Z. Fang, Z.J. Duan, Y. Zhang, S. Chen, *J. Agric. Food. Chem.* 55 (2007) 3869–3876.
- [11] X.B. Luo, Y.C. Zhan, X.M. Tu, Y.N. Huang, S.L. Luo, L.S. Yan, *J. Chromatogr. A* 1218 (2011) 1115–1121.
- [12] E. Caro, R.M. Marcé, P.A.G. Cormack, D.C. Sherrington, F. Borrull, *J. Sep. Sci.* 28 (2005) 2080–2085.
- [13] C. Baggiani, P. Baravalle, G. Giraudi, C. Tozzi, *J. Chromatogr. A* 1147 (2007) 158–164.
- [14] A. Beltran, R.M. Marce, P.A.G. Cormack, F. Borrull, *J. Chromatogr. A* 1216 (2009) 2248–2253.
- [15] K. Mosbach, O. Ramstrom, *Biotechnology* 14 (1996) 163–170.
- [16] Y.H. Zhang, A.J. Tong, L.D. Li, *Spectrochim. Acta* 60 (2004) 241–244.
- [17] B. Selligren, B. Ruckert, A. Hall, *Adv. Mater.* 14 (2002) 1335–1335.
- [18] E. Birlik, A. Ersoz, E. Acikkalp, A. Denizli, R. Say, *J. Hazard. Mater.* 140 (2007) 110–116.
- [19] E. Demirbas, N. Dizge, M.T. Sulak, M. Kobya, *Chem. Eng. J.* 148 (2009) 480–487.
- [20] L. Qin, X.W. He, W. Zhang, W.Y. Li, Y.K. Zhang, *Anal. Chem.* 81 (2009) 7206–7216.
- [21] Z. Reddad, C. Gerente, Y. Andres, P. Cloirec, *Environ. Sci. Technol.* 36 (2002) 2067–2073.